

Effect of coexisting cations on the adsorption of cesium onto poly (β -cyclodextrin)/bentonite composite

Hongjuan Liu^{1,2} · Shuibo Xie^{1,3} · Tiancheng Wang² · Yingjiu Liu³ · Taotao Zeng³

Received: 26 December 2016 / Published online: 5 May 2017
© Akadémiai Kiadó, Budapest, Hungary 2017

Abstract A novel poly(β -cyclodextrin)/bentonite composite (β -CD/BNC) was successfully prepared through graft polymerisation by using ammonium persulphate–sodium bisulphate as initiators, and characterized by FT-IR and EDS. The equilibrium data fit Freundlich isotherm satisfactorily. Adsorption kinetic was fitted with pseudo-second-order. The maximum adsorption capacities for Cs^+ by β -CD/BNC in absence and presence of Na^+ and Mg^{2+} were 48.83 ± 0.35 , 47.30 ± 0.28 , and $42.52 \pm 0.85 \text{ mg g}^{-1}$, respectively. Adsorption of Cs^+ was suppressed by presence of Mg^{2+} more than Na^+ . β -CD/BNC had a higher affinity to Cs^+ than Na^+ and Mg^{2+} . β -CD/BNC was an effective sorbent for the treatment cesium waste water.

Keywords β -CD/BNC · Bentonite · Cs^+ · Coexistent cation · Adsorption

Introduction

^{137}Cs is a serious environmental concern because it is the main nuclear fission product [1]. This substance can be easily released into water during nuclear reactor leaks, such

as those that happened in Chernobyl in 1986 and in Fukushima in 2011 [1–3]. The amount of ^{137}Cs released directly into the sea from the Fukushima accident was approximately $3.5 \pm 0.7 \text{ PBq}$ ($1 \text{ PBq} = 10^{15} \text{ Bq}$) from the end of March to May in 2011 [4]. According to field data obtained from June 4 to 18, 2011, ^{137}Cs released directly into the sea significantly increased the activity and reserves of ^{137}Cs in water near Fukushima [5]. ^{137}Cs is a high heat-release fission product that can penetrate the food chain in the environment. This fission product is a biological hazard with a long half-life of 30.1 years [1, 6–8]. Therefore, cesium should be removed from nuclear waste prior to the discharge to prevent cesium from migrating and diffusing into the environment. Cesium can be removed from waste through adsorption, which is a promising method because of its simplicity and fast adsorption rate [1, 8, 9]. Extensive investigations on the sorption of Cs^+ on different minerals have revealed that this process is mainly dominated by ion-exchange mechanism [9–12].

Bentonite possesses excellent physicochemical properties, such as large specific area, high cation exchange capacity and strong adsorptive affinity for organic and inorganic pollutants [13, 14]. Basing on these advantages, researchers considered bentonite as an excellent adsorbent for wastewater treatment [1, 13, 14]. As such, the sorption behaviours of cesium on bentonite have been widely explored [13–15]. However, the treatment capacity of original bentonite is limited because of its hygroscopic expansion and dispersion in water. Adsorption selectivity and adsorption performance for wastewater treatment should be improved by changing the surface properties and interlayer structure of bentonite. Polymer/bentonite composites have been studied because of their wide applications in environmental protection. For example, polymer/bentonite composites as adsorbents for lead ions have been

✉ Shuibo Xie
xiesbmr@263.net

¹ Key Discipline Laboratory for National Defence for Biotechnology in Uranium Mining and Hydrometallurgy, University of South China, Hengyang 421001, People's Republic of China

² Institute of Nuclear Science and Technology, University of South China, Hengyang 421001, People's Republic of China

³ Hunan Province Key Laboratory of Pollution Control and Resources Reuse Technology, University of South China, Hengyang 421001, People's Republic of China

successfully prepared, and lead ions have been efficiently removed by poly(acrylic acid) with bentonite and polyacrylate with bentonite [16, 17].

β -cyclodextrin (β -CD) possesses a unique structure with a hydrophobic cavity and a hydrophilic outer edge [18]. This molecule can form inclusion complexes with other materials through host–guest phenomena [19, 20]. Compounds with β -CD are characterised by increased sorption values and an ability to combine selectively with some inorganic ions or organic molecules [20]. New CD-based composites have been developed for practical use in the removal of contaminants from wastewater [20, 21]. However, CD derivatives are inapplicable for direct separation and purification purposes because of their solubility in water. Therefore, insoluble CD-based materials should be synthesised by performing polymerisation reactions or by using CD molecules supported on a solid face via grafting [18–21]. β -CD polymers and bentonite are bioabsorbable and biocompatible substances. Our research aimed to synthesise β -CD/bentonite composite (β -CD/BNC) by using epoxy chloropropane as a cross-linker and bentonite as a solid face. Free radicals on bentonite can be formed by initiators, such as ammonium persulphate–sodium bisulphate, because of the presence of several hydroxyl groups on the surface of bentonite. Thus, β -CD/BNC was prepared through grafting polymerisation by free radicals and cross-linking of co-polymers. This composite was also used as a sorbent to remove cesium from an aqueous solution. Cations coexisting in radioactive waste water are important factors affecting the sorbent for Cs^+ removal from the water. Therefore, cesium sorption in the presence of common coexisting cations including monovalent (Na^+) cation and divalent (Mg^{2+}) cation was investigated. Adsorption kinetics, equilibrium isotherms, energy dispersive spectrometer (EDS) and Fourier transform infrared spectroscopy (FT-IR) analyses were conducted to examine the sorption mechanisms and effect of coexistent cations on the adsorption of Cs^+ onto β -CD/BNC.

Materials and methods

Materials

Bentonite obtained from Tianjin was found to be of Ca-type [22]. β -CD was obtained from Kernel Chemical Reagent Co., Ltd, Tianjin, China. Hydrochloric acid, sodium hydroxide, epoxy chloropropane, ammonium persulphate and sodium bisulphate were purchased from Tian Li Chemical Reagent Co., Ltd, Tianjin, China. CsNO_3 was purchased from Fu Chen Chemical Reagent Factory, Tianjin, China. NaNO_3 and $\text{Mg}(\text{NO}_3)_2$ were purchased from Da Mao Chemical Reagent Factory, Tianjin, China.

Preparation of β -CD/BNC

40 g of β -CD added to 120 mL of 40% NaOH aqueous solution was dissolved in a round-bottomed flask at 50 °C and 60 mL of epoxy chloropropane was added dropwise. Afterwards, 30 g of bentonite in 600 mL of water blended into suspension slurry was added, and 1% aqueous solution of ammonium persulphate and sodium bisulphate were added successively. The mixture in the round-bottomed flask was stirred and heated in an electric thermostatic oven at 70 °C for 3 h. After the mixture was cooled to ambient temperature, the reactants were collected through suction filtration by using a vacuum suction filter machine. The crude product was purified by soaking and washing with water and acetone several times, vacuum-dried at 80 °C for 24 h and ground into powder.

Batch adsorption experiment

Effect of contact time and adsorption kinetics, and effect of solution pH, adsorbent dosage, temperature on Cs^+ adsorption by β -CD/BNC in absence and presence of Na^+ and Mg^{2+} was investigated by preparing the final ion concentrations of Cs^+ (100 mg L⁻¹), Cs^+ (100 mg L⁻¹) + Na^+ (100 mg L⁻¹), Cs^+ (100 mg L⁻¹) + Mg^{2+} (100 mg L⁻¹) in 50 mL solution. The effect of contact time and adsorption kinetics of Cs^+ adsorption was studied by keeping the solution with 0.25 g β -CD/BNC under pH 7 at 303 K, and the mixture was sampled at interval. The effect of adsorbent dosage on Cs^+ adsorption was studied by varying the amount of β -CD/BNC from 0.25 to 2 g. The effect of solution pH on Cs^+ adsorption was studied over the range of 3 to 11. The aqueous solution was adjusted into different pH by adding NaOH and HCl. The effect of temperature on Cs^+ adsorption was investigated at 293 K, 303 K and 313 K. During equilibrium isotherms studies, the final concentration of Cs^+ in three groups was brought to 50, 100, 150, 200, 250 mg L⁻¹, respectively, one group without other cation ions, one group with the final concentration of 100 mg L⁻¹ Na^+ and one group with 100 mg L⁻¹ Mg^{2+} , and 0.25 g sample of β -CD/BNC was equilibrated with 50 mL of the spiked solution under neutral pH.

All batch adsorption experiments above were carried out in a glass flask in a air bath shaker (100 r min⁻¹) for 6 h. The solution was separated from the β -CD/BNC particles by filtering through membrane filter and the cesium concentration remaining in the solution was analysed by AA6300 Atomic Absorption Spectrophotometer (AAS). Each adsorption sample of the solution was measured in triplicate, and the average value was used for evaluating the adsorption capacities. In the adsorption tests, the q and K_d of the cesium ions was obtained by using the following equations [22]:

Adsorption capacity $q = V(c_1 - c_2)/m,$ (1)

Distribution capacity $k_d = [V(c_1 - c_2)]/mc_2,$ (2)

where c_1 and c_2 (mg L⁻¹) are the initial ion concentration and the ion concentration after sorption equilibrium, respectively, and V (mL) is the volume of solution, and m (g) is the weight of the solid.

FT-IR and EDS analysis

After adsorption, the FT-IR spectra of β-CD/BNC and β-CD/BNC after adsorption were recorded in KBr pellets at room temperature using a FT-IR spectrometer (Nicolet 6700). The FT-IR samples were analysed in the range of 4000–400 cm⁻¹. The elemental compositions of β-CD/BNC and β-CD/BNC after adsorption were determined by X-Max EDS spectroscopy attached to a JSM-7500F SEM column.

Results and discussion

Effect of contact time and adsorption kinetics

Effect of contact time on Cs⁺ adsorption and sorption kinetics were studied by batch method. Several kinetic models are available to study the sorption mechanism and rate-controlling processes. The pseudo-first order (Eq. 3) and pseudo-second order models (Eq. 4) are the most widely used for representing kinetic data, and they are given as [23, 24]:

$\ln(q_e - q_t) = \ln q_e - k_1 t,$ (3)

$\frac{1}{q_t} = \frac{1}{k_2 q_e^2} = \frac{1}{q_e} t,$ (4)

where q_e and q_t (mg g⁻¹) are the amounts of adsorbed cesium ions on β-CD/BNC at equilibrium and at time t (min), respectively, and k_1 (min⁻¹) is the pseudo-first order sorption rate constant, and k_2 (g mg⁻¹ min⁻¹) is the second-order sorption rate constant.

The adsorption rate of Cs⁺ onto β-CD/BNC in absence and presence of Na⁺ and Mg²⁺ was shown in Fig. 1a. The uptake of Cs⁺ onto β-CD/BNC and adsorption equilibrium was achieved rapidly. The linear forms of the pseudo-first order and the pseudo-second order models for the adsorption of Cs⁺ onto β-CD/BNC are given in Fig. 1b and c, respectively. The linear plots using the pseudo-first order model of Cs⁺ onto β-CD/BNC showed poor correlation ($R^2 < 0.4807$). The pseudo-second order model possessed high correlation coefficients ($R^2 > 0.9998$). This result suggested that the pseudo-first order model was less suitable to describe the adsorption process, and the pseudo-

second order could be adapted to describe the process as it fit accurately with the experimental data. The rapid adsorption kinetics indicated that Cs⁺ sorption of β-CD/BNC was mainly due to chemical rather than physical adsorption [25]. The kinetic constants of the pseudo-second order model were presented in Table 1. According to equilibrium adsorption quantity in Table 1, Na⁺ and Mg²⁺ could reduce the equilibrium adsorption quantity of Cs⁺ onto β-CD/BNC, and the effect of Mg²⁺ on the adsorption of Cs by β-CD/BNC was greater than that of Na⁺. The reasons might be as follows: (1) competitive cations (Na⁺ and Mg²⁺) occupy the adsorption vacancies on the surface of β-CD/BNC, which leads to Cs⁺ adsorption capacity decreased; (2) The ion exchange is one of the adsorption mechanisms of Cs⁺ onto β-CD/BNC. Ion exchange competition of Mg²⁺ and Na⁺ could inhibited the exchange adsorption between Cs⁺ and β-CD/BNC, and the cation exchange capacity of Mg²⁺ onto β-CD/BNC was greater than that of Na⁺.

Equilibrium isotherm studies

To obtain a better understanding of Cs⁺ sorption mechanism and to quantify the sorption data, Langmuir and Freundlich models are adopted to fit the sorption isotherms and to simulate the experimental data [26–28]. The Langmuir isotherm model is expressed by the following equation [22, 26]:

$q = q_{max} K_L c / (1 + K_L c).$ (5)

Equation (5) can be expressed in linear form:

$\frac{1}{q} = \frac{1}{q_{max}} + \frac{1}{K_L q_{max}} \times \frac{1}{c},$ (6)

where c (mg L⁻¹) is the equilibrium concentration of Cs⁺ in solution; q (mg g⁻¹) is the amount of Cs⁺ adsorbed per weight unit of β-CD/BNC after equilibrium; q_{max} (mg g⁻¹) represents the maximum sorption amount and K_L (L mg⁻¹) is a constant related to the enthalpy of sorption.

The Freundlich isotherm model is usually expressed as follows [22, 26]:

$q = K_F c^{\frac{1}{n}}.$ (7)

Equation (7) can be expressed in linear form

$\ln q = \frac{1}{n} \ln c + \ln K_F,$ (8)

where K_F (L mg⁻¹) represents the adsorption capacity as Cs⁺ equilibrium concentration is 1; n is the adsorption performance of adsorbents with equilibrium concentration.

The Langmuir and Freundlich isotherms of β-CD/BNC for Cs⁺ at 30 °C were indicated in Fig. 2a and b, and the parameters of the isotherm models were showed in

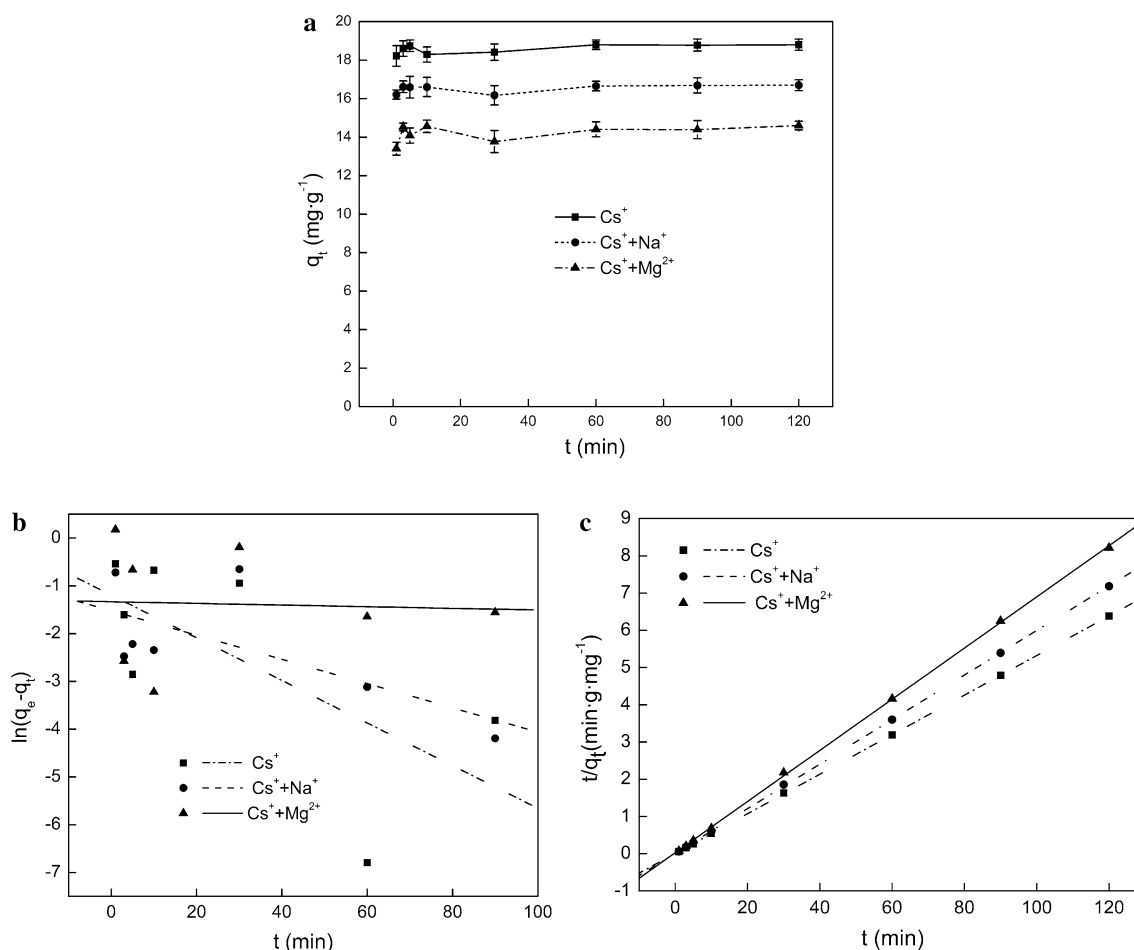


Fig. 1 Adsorption kinetics of Cs onto β -CD/BNC in absence and presence of Na^+ and Mg^{2+} (**a** sorption with different contact time; **b** pseudo-first order sorption kinetic; **c** pseudo-second order sorption kinetic)

Table 1 Kinetic constants of pseudo-second order model and correlation coefficients (R^2) of Cs^+ onto β -CD/BNC

Adsorbate	Fitting equation	Corresponding parameters
Cs^+	$t/q_t = 0.00909 + 0.05314t$	$q_e = 18.82 \pm 0.37 \text{ mg g}^{-1}$, $k = 0.311 \pm 0.019 \text{ g (mg}^{-1} \text{ min}^{-1})$, $R^2 = 0.9999$
$\text{Cs}^+ + \text{Na}^+$	$t/q_t = 0.01122 + 0.05985t$	$q_e = 16.71 \pm 0.43 \text{ mg g}^{-1}$, $k = 0.319 \pm 0.025 \text{ g (mg}^{-1} \text{ min}^{-1})$, $R^2 = 0.9999$
$\text{Cs}^+ + \text{Mg}^{2+}$	$t/q_t = 0.02619 + 0.06872t$	$q_e = 14.55 \pm 0.81 \text{ mg g}^{-1}$, $k = 0.180 \pm 0.010 \text{ g (mg}^{-1} \text{ min}^{-1})$, $R^2 = 0.9998$

Table 2. The Langmuir and Freundlich models had a good fit with the experimental data, and the Freundlich models was a better fit on the basis of R^2 listed in Table 2. The maximum adsorption capacity for Cs^+ by β -CD/BNC was $48.83 \pm 0.35 \text{ mg g}^{-1}$ (Cs^+), $47.30 \pm 0.28 \text{ mg g}^{-1}$ ($\text{Cs}^+ + \text{Na}^+$), and $42.52 \pm 0.85 \text{ mg g}^{-1}$ ($\text{Cs}^+ + \text{Mg}^{2+}$), respectively. The values of n ($1 < n < 10$) indicated that the adsorption of Cs^+ by β -CD/BNC was favourable. K_L and K_F in Table 2 offered estimates about the adsorption capacity of β -CD/BNC. K_L and K_F ($\text{Cs}^+ > \text{Cs}^+ + \text{Na}^+ > \text{Cs}^+ + \text{Mg}^{2+}$) of β -CD/BNC in Table 2 indicated

that Na^+ and Mg^{2+} could reduce the adsorption capacity of Cs^+ onto β -CD/BNC and the effect of Mg^{2+} on the adsorption was greater than that of Na^+ . Even though, β -CD/BNC had a higher affinity to Cs^+ than the competitive cations (Na^+ and Mg^{2+}), which showed that β -CD/BNC was an effective adsorbent for Cs^+ .

Effect of adsorbent dosage

Effect of β -CD/BNC adsorbent dosage on the adsorptive capacity of Cs^+ in absence and presence of Na^+ and Mg^{2+}

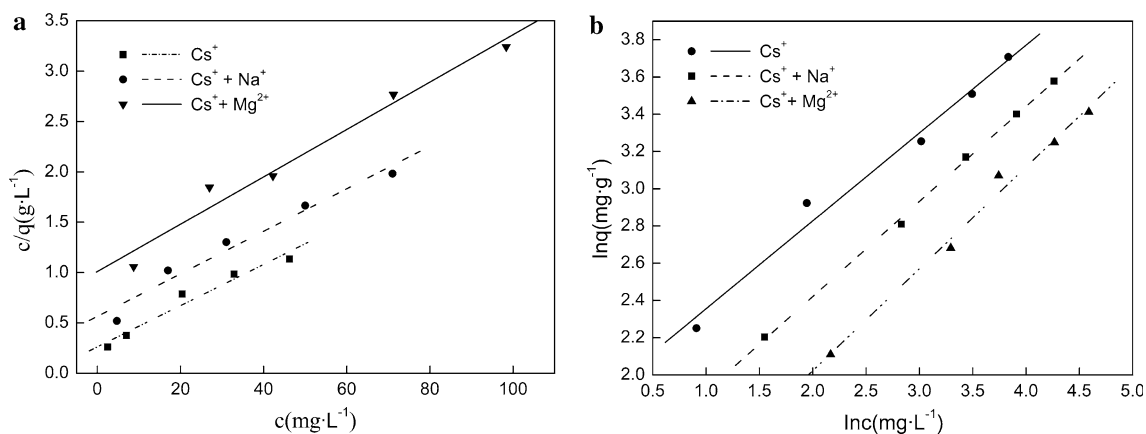


Fig. 2 Langmuir isotherms (a) and Freundlich isotherms (b) of Cs⁺ onto β-CD/BNC in absence and presence of Na⁺ and Mg²⁺

Table 2 Langmuir and Freundlich models parameters of Cs⁺ onto β-CD/BNC

Models	Adsorbate	Fitting equation	Corresponding parameters
Langmuir	Cs ⁺	$c/q = 0.26216 + 0.02048c$	$R^2 = 0.9598, Q_m = 48.83 \pm 0.35 \text{ mg g}^{-1}, k_L = 0.078 \pm 0.043 \text{ L mg}^{-1}$
	Cs ⁺ + Na ⁺	$c/q = 0.5645 + 0.02114c$	$R^2 = 0.9640, Q_m = 47.30 \pm 0.28 \text{ mg g}^{-1}, k_L = 0.037 \pm 0.012 \text{ L mg}^{-1}$
	Cs ⁺ + Mg ²⁺	$c/q = 1.01047 + 0.02352c$	$R^2 = 0.9722, Q_m = 42.52 \pm 0.85 \text{ mg g}^{-1}, k_L = 0.023 \pm 0.009 \text{ L mg}^{-1}$
Freundlich	Cs ⁺	$\ln q = 1.88401 + 0.47176 \ln c$	$R^2 = 0.9830, n = 2.120 \pm 0.061, k_F = 6.580 \pm 0.123$
	Cs ⁺ + Na ⁺	$\ln q = 1.40028 + 0.51043 \ln c$	$R^2 = 0.9985, n = 1.959 \pm 0.022, k_F = 4.056 \pm 0.151$
	Cs ⁺ + Mg ²⁺	$\ln q = 0.93026 + 0.54663 \ln c$	$R^2 = 0.9887, n = 1.829 \pm 0.034, k_F = 2.535 \pm 0.080$

was showed in Fig. 3. It was obvious that the adsorptive capacity of Cs⁺ in absence and presence of Na⁺ and Mg²⁺ decreased with an increasing amount of β-CD/BNC from 0.25 to 2 g. This could be because more active sites were offered by an increasing amount of β-CD/BNC, which allowed more sorption points of Cs⁺. However, too many adsorption sites led to unsaturated adsorption on the surface of β-CD/BNC adsorbent, so the adsorption capacity per unit weight of adsorbent decreased. From Fig. 3, we can see that Na⁺ and Mg²⁺ have little effect on cesium adsorption when adsorbent dosage increased to 1–2 g. This may be due to unsaturated adsorption on the surface of β-CD/BNC, and more adsorption sites were provided for Na⁺ and Mg²⁺ to reduced their competition with Cs⁺.

Effect of solution pH

The solution pH is a very important parameter for the adsorption of Cs⁺ onto β-CD/BNC. The effect of pH on the adsorptive capacity of Cs⁺ onto β-CD/BNC in absence and presence of Na⁺ and Mg²⁺ was indicated in Fig. 4. The adsorption capacity for the cesium ions increased with an increase of solution pH in the range of 3 and 11. The results were speculated that it could be attributed to a change in the surface charge of β-CD/BNC [14]. Electrostatic

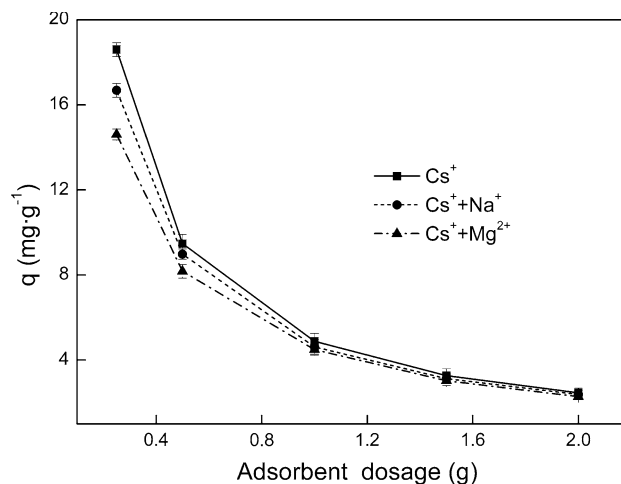


Fig. 3 Effect of adsorbent dosage on the Cs⁺ sorption in 50 mL solution absence and presence of Na⁺ and Mg²⁺, temperature 303 K, pH 7

attraction such as an ion exchange reaction between cesium ion and β-CD/BNC was one of dynamic adsorption [14]. The surface charge of β-CD/BNC could increased negatively with the increase of solution pH, which might cause an increase of the adsorptive capacity by the electrostatic adsorption. This conclusion was similar to that reported in

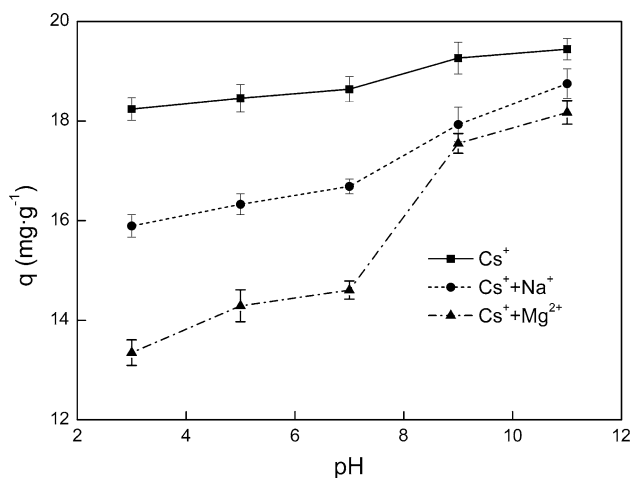


Fig. 4 Effect of solution pH on the Cs^+ sorption in 50 mL solution absence and presence of Na^+ and Mg^{2+} , temperature 303 K, adsorbent dosage 0.25 g

previous literature [14, 22]. In presence of Mg^{2+} in the solution, Mg^{2+} have littler effect on cesium adsorption when solution pH increased to 9–11. This may be because Mg^{2+} produced precipitation in the alkaline solution and reduced its competition with Cs^+ .

Effect of temperature and adsorption thermodynamic

Figure 5 showed the effect of temperature on q of Cs^+ sorption by $\beta\text{-CD/BNC}$ in absence and presence of Na^+ and Mg^{2+} . The q of Cs^+ sorption increased with an increasing temperature from 293 to 313 K. The results indicated that the adsorption process was endothermic. The values of thermodynamic parameters (ΔS^0 , ΔH^0 and ΔG^0) of the adsorption reaction were determined subsequently by using the the following equations [29, 30]:

$$\ln K_d = \frac{-\Delta H^0}{RT} + \frac{\Delta S^0}{R}, \quad (9)$$

$$\Delta G^0 = \Delta H^0 - T\Delta S^0, \quad (10)$$

where T is absolute temperature (K), R is the ideal gas constant [$8.314 \text{ (J mol}^{-1} \text{ K}^{-1})$], and K_d is the distribution coefficient of cesium (mL g^{-1}). The intercept of the linear line of $\ln K_d$ versus $1/T$ (Fig. 6) by the van't Hoff equation (Eq. (9)). The values of thermodynamic parameters were shown in the Table 3.

The values of ΔG^0 were negative at the temperature from 293 to 313 K, which confirmed the spontaneous nature of the adsorption [30]. The negative values of ΔG^0 increasing with a increase of the temperature indicated greater Cs^+ adsorption capacity of $\beta\text{-CD/BNC}$ at the higher temperature. The positive values of ΔH^0 revealed the endothermic nature of Cs^+ adsorption by $\beta\text{-CD/BNC}$. The

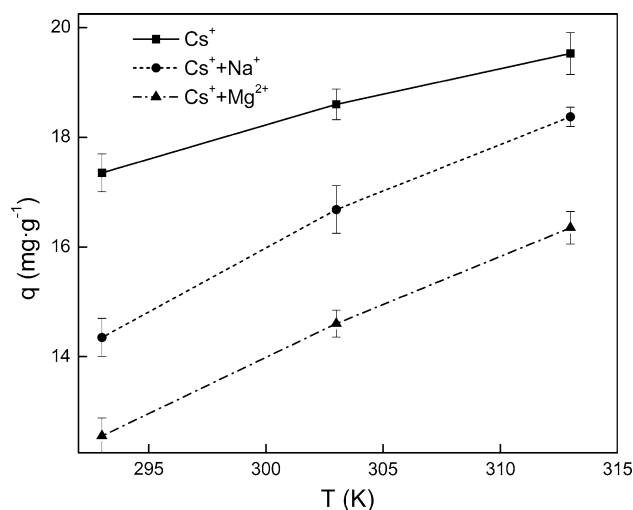


Fig. 5 Effect of temperature on the Cs^+ sorption in 50 mL solution absence and presence of Na^+ and Mg^{2+} , adsorbent dosage 0.25 g, pH 7

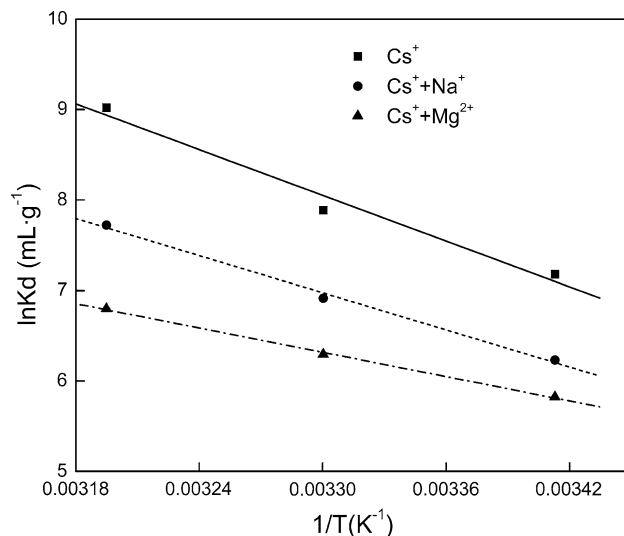


Fig. 6 A liner plot of $\ln K_d$ versus $1/T$ of Cs^+ sorption by $\beta\text{-CD/BNC}$ in 50 mL solution absence and presence of Na^+ and Mg^{2+}

positive values of ΔS^0 implied an increase of the randomness at the $\beta\text{-CD/BNC/solution}$ interface during the cesium adsorption.

FT-IR analysis

The FT-IR spectra of bentonite, $\beta\text{-CD}$, $\beta\text{-CD/BNC}$ and $\beta\text{-CD/BNC}$ after adsorption were shown in Fig. 7. The bentonite spectra in Fig. 7a was previously described in our study [22]. From Fig. 7a and c, the surface structure of bentonite has been changed after polymerisation with $\beta\text{-CD}$. The peak at 3627 cm^{-1} of bentonite due to the Al–O–H stretch [22] disappeared on $\beta\text{-CD/BNC}$, which was due

Table 3 Thermodynamic parameters of Cs⁺ onto β-CD/BNC in absence and presence of Na⁺ and Mg²⁺

Adsorbate	Temperature (K)	ΔG ⁰ (KJ mol ⁻¹)	ΔH ⁰ (KJ mol ⁻¹)	ΔS ⁰ (J mol ⁻¹ K ⁻¹)
Cs ⁺	293	-87.32 ± 0.67	70.10 ± 0.83	298.26 ± 1.29
	303	-90.30 ± 0.95		
	313	-93.29 ± 1.36		
Cs ⁺ + Na ⁺	293	-71.878 ± 0.43	56.83 ± 0.71	245.52 ± 0.98
	303	-74.33 ± 0.72		
	313	-76.79 ± 0.89		
Cs ⁺ + Mg ²⁺	293	-51.36 ± 0.35	37.24 ± 0.69	175.40 ± 0.85
	303	-53.11 ± 0.78		
	313	-54.86 ± 0.41		

to the effect between Al–O–H of bentonite and epoxy chloropropane. The characteristic peaks of β-CD at approximately 2925 and 1413 cm⁻¹ (Fig. 7b) that corresponded to the C–H and CH₂– stretching vibration, respectively, was added and shifted into β-CD/BNC at approximately 2976 and 1420 cm⁻¹ [31]. It indicated that β-CD was grafted onto the bentonite after the polymerisation reaction.

In Fig. 7c and d, the FT-IR spectra presented the spectrum change of β-CD/BNC before and after cesium sorption. After adsorption was completed (Fig. 7d), the transmittance raised with cesium sorption, and the intensity of several characteristic peaks of β-CD/BNC was enhanced. The peak of β-CD/BNC at 3430 cm⁻¹ corresponding to H–O–H stretch was shifted to 3423 cm⁻¹. This indicated that H–O–H group of the β-CD/BNC might take part in the cesium sorption. Figure 7c and e indicated the change of the FT-IR spectrum of β-CD/BNC before and after Cs⁺ + Na⁺ adsorption. It showed that the transmittance weakened, some characteristic peaks of β-CD/BNC were shifted and the peaks of β-CD/

BNC at 3430 and 1637 cm⁻¹ were shifted to 3380 and 1654 cm⁻¹ after Cs⁺ + Na⁺ adsorption. From Fig. 7d and e, comparing with the adsorption of Cs⁺ without Na⁺, we observed that more functional groups on the surface of β-CD/BNC participated in the adsorption reaction when competition with Na⁺ existed. Figure 7c and f indicated the change of the FT-IR spectrum of β-CD/BNC before and after Cs⁺ and Mg²⁺ adsorption. After Cs⁺ + Mg²⁺ adsorption, the peak of β-CD/BNC at 3430 cm⁻¹ was also shifted to 3423 cm⁻¹, which had the same change in the Cs⁺ adsorption without Mg²⁺. From Fig. 7d and f, the change of the functional groups on the surface of β-CD/BNC after Cs⁺ + Mg²⁺ adsorption was similar to that after Cs⁺ adsorption without Mg²⁺. This showed that the effect of Mg²⁺ on the adsorption of Cs⁺ might mainly inhibit ion-exchange adsorption between Cs⁺ and β-CD/BNC, rather than compete with Cs⁺ for the functional groups of β-CD/BNC.

EDS analysis

The compositions of β-CD/BNC and β-CD/BNC after adsorption were estimated from EDS measurements (shown in Fig. 8a–d). Comparing with the EDS spectrum of bentonite (analysed in our previous study) [22] and β-CD/BNC, the researchers observation of the presence of C (10.66%) peaks and increase of O (from 51.53 [22] to 55.29%) confirmed that β-CD was grafted onto the bentonite during polymerisation. As shown in Fig. 8b, the increase of Cs peak after Cs⁺ adsorption in the EDS pattern confirmed that cesium ions were adsorbed by β-CD/BNC. From Fig. 8b, c and d, Cs in β-CD/BNC was 1.77% after Cs⁺ adsorption, 1.37% after Cs⁺ + Na⁺ adsorption and 1.21% after Cs⁺ + Mg²⁺ adsorption, which further proved that Na⁺ and Mg²⁺ could reduce Cs⁺ sorption by β-CD/BNC, and the Cs⁺ sorption was suppressed by presence of Mg²⁺ more than Na⁺. Ca in β-CD/BNC was 2.40%, 2.17% after Cs⁺ adsorption, 2.00% after Cs⁺ + Na⁺ adsorption and 0.75% after Cs⁺ + Mg²⁺ adsorption. The results

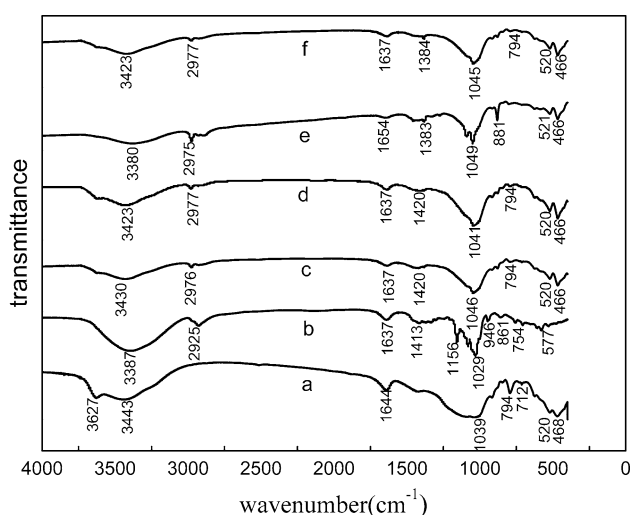


Fig. 7 FT-IR spectra of bentonite (a), β-CD (b), β-CD/BNC (c), β-CD/BNC after Cs⁺ adsorption (d), β-CD/BNC after Cs⁺ + Na⁺ adsorption (e) and β-CD/BNC after Cs⁺ + Mg²⁺ adsorption (f)

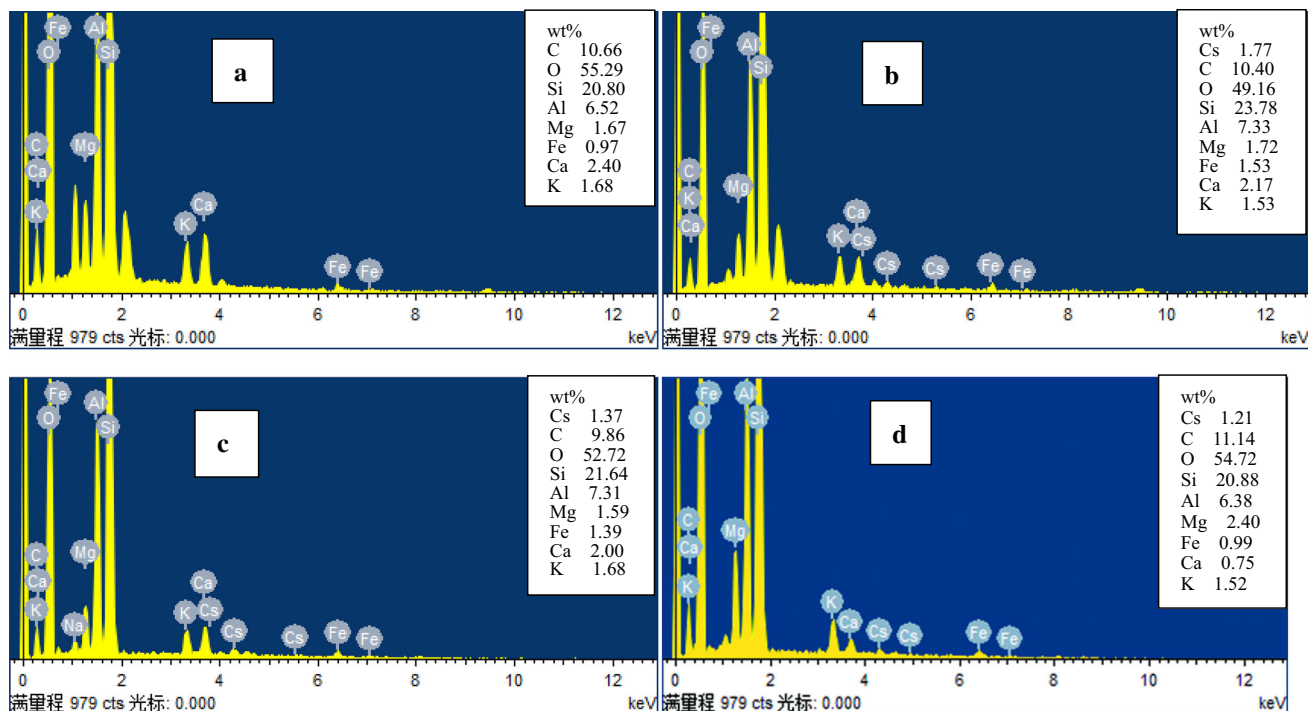


Fig. 8 EDS spectrum of β -CD/BNC (a), β -CD/BNC after Cs^+ adsorption (b), β -CD/BNC after $\text{Cs}^+ + \text{Na}^+$ adsorption (c) and β -CD/BNC after $\text{Cs}^+ + \text{Mg}^{2+}$ adsorption (d)

indicated that Cs^+ , Na^+ , and Mg^{2+} in aqueous solution were exchanged for the interlayer hydration cations (Ca^{2+}) of β -CD/BNC by ion exchange reaction. Cs^+ sorption in the presence of Mg^{2+} , Ca in β -CD/BNC decreased more obviously (from 2.4 to 0.75%), which showed the influence of Mg^{2+} on adsorption of Cs was mainly due to competitive ion exchangeable reaction with Ca in β -CD/BNC. This result further confirmed the FT-IR result shown above.

Conclusions

The equilibrium data and adsorption kinetic data of the adsorption of Cs^+ onto β -CD/BNC in absence and presence of Na^+ and Mg^{2+} fit Freundlich isotherm and pseudo-second-order kinetic models, respectively. Thermodynamic parameters indicated that the adsorption process were spontaneous and endothermic nature. Competitive cations (Na^+ and Mg^{2+}) could reduce the adsorption capacity of Cs^+ onto β -CD/BNC, and the effect of Mg^{2+} on the adsorption of Cs^+ by β -CD/BNC was greater than that of Na^+ . β -CD/BNC was preferential adsorption toward Cs^+ than competitive cations (Na^+ and Mg^{2+}). More functional groups on the surface of β -CD/BNC participated in adsorption when Na^+ competed with Cs^+ . The effect of Mg^{2+} on the adsorption of Cs^+ mainly inhibit ion exchange adsorption between Cs^+ and β -CD/BNC rather than compete with Cs^+ for the

functional groups of β -CD/BNC. Mg^{2+} on adsorption of Cs was mainly due to competitive ion exchangeable reaction with Ca in β -CD/BNC. The results of our study showed that β -CD/BNC was an effective sorbent for cesium.

Acknowledgements This work was supported by the Doctoral Fund of High Education Program (Grant No. 20134324110003), the National Natural Science Foundation of China (Grant No. 11475080), the General Program of the Hunan Provincial Education Department (Grant No. 15C1178), the Graduate Student Research Innovation Project of Hunan Province (CX2016B427).

References

1. Yang SB, Hanc C, Wang XK, Nagatsua M (2014) Characteristics of cesium ion sorption from aqueous solution on bentonite- and carbon nanotube-based composites. *J Hazard Mater* 274:46–52
2. Sawidis T, Tsigaridas K, Tsikritzis L (2010) Cesium-137 monitoring using lichens from W. Macedonia, N. Greece. *Ecotox Environ Safe* 73(7):1789–1796
3. Tateda Y, Tsumune D, Tsubono T (2013) Simulation of radioactive cesium transfer in the southern Fukushima coastal biota using a dynamic food chain transfer model. *J Environ Radioact* 124(5):1–12
4. Tsumune D, Tsubono T, Aoyama M, Hirose K (2012) Distribution of oceanic ^{137}Cs from the Fukushima Daiichi Nuclear Power Plant simulated numerically by a regional ocean model. *J Environ Radioact* 111:100–108
5. Buesseler KO, Jayne SR, Fisher NS, Rypina I, Baumann H, Baumann Z (2012) Fukushima-derived radionuclides in the ocean and biota off Japan. *Proc Natl Acad Sci USA* 109:5984–5988

6. Li TT, He F, Dai YD (2016) Prussian blue analog caged in chitosan surface-decorated carbon nanotubes for removal cesium and strontium. *J Radioanal Nucl Chem* 310(3):1139–1145
7. Mao XY, Han FXX, Shao XH, Guo K, McComb J, Arslan Z, Zhang ZY (2016) Electro-kinetic remediation coupled with phytoremediation to remove lead, arsenic and cesium from contaminated paddy soil. *Ecotox Environ Safe* 125:16–24
8. Dwivedi C, Kumar A, Ajish JK, Singh KK, Kumar M, Wattal PK, Bajaj PN (2012) Resorcinol–formaldehyde coated XAD resin beads for removal of cesium ions from radioactive waste: synthesis, sorption and kinetic studies. *RSC Adv* 2:5557–5564
9. Endo M, Yoshikawa E, Muramatsu N, Takizawa N, Kawai T, Unuma H, Sasaki A, Masano A, Takeyama Y, Kahara T (2013) The removal of cesium ion with natural Itaya zeolite and the ion exchange characteristics. *J Chem Technol Biotechnol* 88(9):1597–1602
10. Borai EH, Harjula R, Malinen L, Paaanen A (2009) Efficient removal of cesium from low level radioactive liquid waste using natural and impregnated zeolite minerals. *J Hazard Mater* 172(1):416–422
11. Avramenko V, Bratskaya S, Zhelezov V, Sheveleva I, Viotenko O, Sergienko V (2011) Colloid stable sorbents for cesium removal preparation and application of latex particles functionalized with transition metals ferrocyanides. *J Hazard Mater* 186(2/3):1343–1350
12. Ding N, Kanatzidis MG (2010) Selective incarceration of cesium ions by Venus flytrap action of a flexible framework sulphide. *Nat Chem* 2:187–191
13. Galamboš M, Kufčáková J, Rajec P (2009) Adsorption of cesium on domestic bentonites. *J Radioanal Nucl Chem* 281:485–492
14. Lee JO, Cho WJ, Choi H (2013) Sorption of cesium and iodide ions onto KENTEX-bentonite. *Environ Earth Sci* 70(5):2387–2395
15. Belkhir S, Guerza M, Chouik S, Boucheffa Y, Mekhalif Z, Delhalle J, Colella C (2012) Textural and structural effects of heat treatment and irradiation on Cs-exchanged NaX zeolite, bentonite and their mixtures. *Microporous Mesoporous Mater* 161:115–122
16. He YF, Zhang L, Yan DZ, Liu SL, Wang H (2012) Poly(acrylic acid) modifying bentonite with in situ polymerisation for removing lead ions. *Water Sci Technol* 65(8):1383–1391
17. He Y, Pei M, Xue N, Wang L, Guo W (2016) Synthesis of sodium polyacrylate–bentonite using in situ polymerisation for Pb²⁺ removal from aqueous solutions. *Rsc Adv* 6(53):48145–48154
18. Xavier CR, Silva APC, Schwingel LC, Borghetti GS, Koester LS (2010) Improvement of genistein content in solid genistein/ β -cyclodextrin complexes. *Quim Nova* 33(3):511–521
19. Namazi H, Heydari A (2014) Synthesis of β -cyclodextrin-based dendrimer as a novel encapsulation agent. *Polym Int* 63:1447–1455
20. Namazi H, Heydari A, Pourfarzolla A (2014) Synthesis of glycoconjugated polymer based on polystyrene and nanoporous β -cyclodextrin to remove copper (II) from water pollution. *Int J Polym Mater Polym Biomater* 63(1):1–6
21. Heydari A, Sheibani H (2015) Fabrication of poly (β -cyclodextrin-co-citric acid)/bentonite clay nanocomposite hydrogel: thermal and absorption properties. *Rsc Adv* 5:82438–82449
22. Liu HJ, Xie SB, Xia LS, Tang Q, Kang X, Huang F (2016) Study on adsorptive property of bentonite for cesium. *Environ Earth Sci* 75(2):1–7
23. Qing YH, Li J, Kang B, Chang SQ, Dai YD, Long Q, Yuan C (2015) Selective sorption mechanism of Cs⁺ on potassium nickel hex-acyanoferrate(II) compounds. *J Radioanal Nucl Chem* 304(2):527–533
24. Saini AS, Melo JS (2015) Biosorption of uranium by human black hair. *J Environ Radioact* 142:29–35
25. Sun Y, Wang Q, Chen C, Tan X, Wang X (2012) Interaction between Eu(III) and graphene oxide nanosheets investigated by batch and extended X-ray absorption fine structure spectroscopy and by modeling techniques. *Environ Sci Technol* 46(11):6020–6027
26. Ismail IM, El-Sourougy MR, Moneim NA, Aly HF (1999) Equilibrium and kinetic studies of the sorption of cesium by potassium nickel hexacyanoferrate complex. *J Radioanal Nucl Chem* 240(1):59–67
27. Wang JS, Hu XJ, Liu YG, Xie SB, Bao ZL (2010) Biosorption of uranium (VI) by immobilized beads. *J Environ Radioact* 101:504–508
28. Xiao J, Chen YT, Zhao WH, Xu JB (2013) Sorption behavior of U(VI) onto Chinese bentonite: effect of pH, ionic strength, temperature and humic acid. *J Mol Liq* 188:178–185
29. Liu SJ, Li S, Zhang HX, Wu LP, Sun L (2016) Ma JG (2016) Removal of uranium(VI) from aqueous solution using graphene oxide and its amine-functionalized composite. *J Radioanal Nucl Chem* 309(2):607–614
30. Zong YL, Zhang YD, Lin XY, Ye D, Luo XG, Wang J (2017) Preparation of a novel microsphere adsorbent of prussian blue encapsulated in carboxymethyl cellulose sodium for Cs(I) removal from contaminated water. *J Radioanal Nucl Chem* 311(3):1577–1591
31. Chalasani R, Vasudevan S (2012) Cyclodextrin functionalized magnetic iron oxide nanocrystals: a host-carrier for magnetic separation of non-polar molecules and arsenic from aqueous media. *J Mater Chem* 22(30):14925–14931